Date of publication xxxx 00, 0000, date of current version xxxx 00, 0000.

Digital Object Identifier 10.1109/ACCESS.2017.DOI

A Kalman based Hybrid Precoding for Multi-User Millimeter Wave MIMO Systems

ANNA VIZZIELLO[1], (Member, IEEE), PIETRO SAVAZZI[1], (Senior Member, IEEE), and KAUSHIK R. CHOWDHURY[2], (Senior Member, IEEE)

[1]Department of Electrical, Computer and Biomedical Engineering, University of Pavia, 27100, Pavia, Italy (e-mail: given name.surname@unipv.it)
[2]Department of Electrical and Computer Engineering, Northeastern University, Boston MA 02115, USA (e-mail: krc@ece.neu.edu)

Corresponding author: Anna Vizziello (e-mail: anna.vizziello@unipv.it).

This work is supported in part by MathWorks under the Development-Collaboration Research Grant on "Cross-layer approach to 5G wireless communications".

ABSTRACT Millimeter wave (mmWave) communication in the 60 GHz band requires large antenna arrays at both the transmit and receive terminals to achieve beamforming gains, in order to counteract the high pathloss. Fully digital techniques are infeasible with large antenna arrays due to hardware constraints at such frequencies, while purely analog solutions suffer severe performance limitations. Hybrid analog/digital beamforming is a promising solution, especially when extended to a multi-user scenario. This paper conveys three main contributions: (i) a Kalman-based formulation for hybrid analog/digital precoding in multi-user environment is proposed, (ii) an analytical expression of the error between the transmitted and estimated data is formulated, so that the Kalman algorithm at the base station (BS) does not require information on the estimated data at the mobile stations (MSs), and instead, relies only on the precoding/combining matrix, (iii) an iterative solution is designed for the hybrid precoding scheme with affordable complexity. Simulation results confirm significant improvement of the proposed approach in terms of both BER and spectral efficiency- achieving almost 7 bps/Hz, at 20 dB with 10 channel paths with respect to the analog-only beamsteering, and almost 1 bps/Hz with respect to the hybrid minimum mean square error (MMSE) precoding under the same conditions.

INDEX TERMS Hybrid beamforming, Kalman filter, Millimiter Wave, massive MIMO

I. INTRODUCTION

Millimeter wave (mmWave) band communication is a key enabling technology for solving the spectrum crunch in future 5G systems [1]–[7]. Due to limited available spectrum in the sub-6GHz band, conventional cellular and WiFi-based solutions cannot be scaled up to meet the ever-growing data demands of network densification, and emerging applications associated with data centers and mobile devices. While innovative solutions such as utilizing licensed spectrum on an opportunistic basis have been proposed [8], such approaches are still subjected to frequent disruption and are limited by the channel bandwidth available in the licensed bands, such as the TV bands. Millimeter wave (mmWave) band communication in the recently opened up contiguous block of unlicensed spectrum in the 57-71GHz range is an opportunity for achieving gigabit-per-second data rates [9]. Indeed, existing standards like the IEEE 802.11ad operating in these bands allow up to 2GHz-wide channels for short-distance communications.

• **MmWave challenges:** Due to the high path loss characterizing mmWave bands, directional beamforming exploiting large antenna arrays at both base station (BS) and mobile stations (MSs) is required [10]–[13]. This enables high quality and long-distance communication links, and increases the signal power concentrated at the receiver end. The high frequency of operation also supports massive multi-antenna architectures from a design viewpoint, while reducing the size of each antenna and allowing many of them to be packed in a small area.

While the hardware support from large antenna arrays for beamforming functions is already available, the high frequency of operation, expected sampling rates and channel bandwidths make it difficult to deploy traditional fully digital beamforming solutions [10], [14]. Thus, analog beamform-

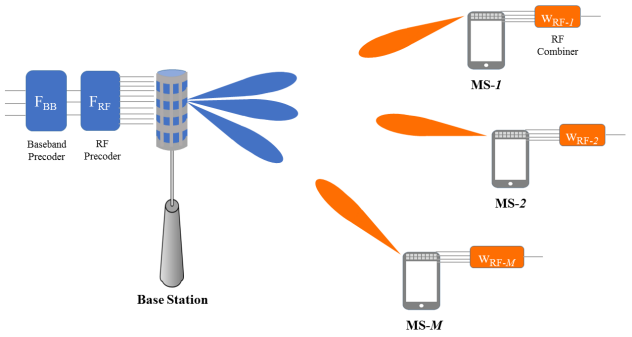

FIGURE 1. MmWave multi-user system model: BS hybrid analog/digital precoding and MS analog combining.

ing techniques is a possible alternative in mmWave systems, such as [15]–[19], which coordinate the signal phases of the antennas through analog phase shifters.

However, analog solutions cannot use adaptive gain control. Moreover, phase shifters can be digitally controlled with only quantized phases [12], thus limiting the possibility of advanced processing and resulting in poor performance. For example, our experiments prove that analog beamforming may achieve at most a spectral efficiency around 3 bps/Hz at 20 dB, while our proposed hybrid analog/digital beamforming gets 10 bps/Hz under the same conditions.

In summary, hybrid schemes are promising candidate solutions that overcome the limitations of pure digital or analog beamforming, as they incorporate the advantages of both methods [20], [21]. Hybrid schemes reduce the training overhead compared to analog-only architectures by leveraging multiple simultaneous beam transmissions. In hybrid solutions, the number of RF chains may be much lower than the number of antennas [1], thus reducing the complexity compared to fully digital solutions. It also allows more freedom than classical analog beamforming by dividing the multiple input multiple output (MIMO) optimization process between analog and digital domains. An advantage of the hybrid approach is that the digital precoder/combiner can compensate for lack of precision in the analog domain, for e.g., it can cancel residual multi-stream interference [1]. In particular, hybrid precoding/combining signals for a single-user has been analyzed for mmWave systems [10], [22]–[25], showing that hybrid designs are able to achieve similar performance compared to fully digital solutions. As an example, the hybrid solution [10] decomposes the optimal precoding and combining matrix via an orthogonal matching pursuit, where the transmit and receive response vectors represent the basis vectors. However, to sustain many simultaneously active BS-MS links, suitable for multi-user mmWave systems where BS and MSs form multiple beams, new solutions need to be developed for inter-user interference reduction.

• **Current hybrid multi-user mmWave solutions:** Multi-user solutions for sub-6GHz channels [26], [27], cannot be directly applied since they do not consider hardware constraints and the specific mmWave channel features. Furthermore, given the difficulty in processing samples timely in these bands, low-complexity solutions must be emphasized.

There are several previous solutions for hybrid multi-user mmWave systems [12], [28]–[34]. The authors in [12] propose a two-stage hybrid precoding scheme. First, as in the single-user scheme, the BS and the MS jointly select a 'best' combination of radio frequency (RF) beamformer and RF combiner in order to maximize the channel gain to that specific MS. Then, a zero-forcing (ZF) baseband precoding algorithm is applied at the BS by inverting the effective channel, in order to reduce the interference between the users. Also [28] uses a digital ZF baseband precoder. While [12] requires explicit channel state information (CSI) feedback from users, [28] develops a non-feedback non-iterative channel estimation. Specifically, the strongest angle of arrivals (AoAs) at both BS and users are estimated, which are exploited for analog beamforming at BS and MSs. Then, the MSs send orthogonal pilot symbols to the BS along the strongest AoA directions to ease the equivalent channel estimation used in the BS digital ZF precoder.

[29] first configures the RF combiner for each MS independently, and then designs the RF and baseband precoder at the BS for all the MSs jointly. The analog/digital precoder minimizes the mean-squared error (MSE) of the data streams received at the MSs. Also other solutions include minimum mean square error (MMSE) as a part of the approach. In particular, an iterative algorithm for joint precoding and combining is proposed in [30]. At the initial step, the analog precoder/combiner is selected through an orthogonal matching pursuit (OMP) algorithm to enhance the channel gain, while mitigating the multi-user interference, and the digital combiner is obtained via MMSE criterion. Then, the iterative procedure is applied to improve the performance. In [31], the authors first develop the digital precoder/combiner leveraging minimum sum-mean-square-error (min-SMSE) criterion to minimize the BER, and then design an over-sampling codebook (OSC) based analog precoder/combiner scheme to further reduce the SMSE. [32] handles the inter-user interference at both analog and digital beamforming levels as follows: the analog beamforming matrix is calculated through the low complexity Gram-Schmidt algorithm and the digital matrix is obtained by the MMSE method with a low dimensional effective channel.

Block diagonalization solutions include methods as those described in [33], [34]. Specifically, in [33] phase-only RF precoding and combining is performed exploiting the large array gain, and then the block diagonalization method is applied at the equivalent baseband channel. The algorithm [34] designs an hybrid beamforming in two steps: first it finds an equivalent baseband channel by maximizing its capacity through the analog RF processing, then the interference among the users is mitigated by the block diagonalization procedure.

Prior works have developed algorithms to maximize the spectral efficiency rather than to minimize the bit error rate

(BER) performance [12], [28]–[30], [32]–[34]. Few BER optimization solutions include works such as [31], [35]. To the best of our knowledge, this is the first work that designs a hybrid precoder for mmWave multi-user massive MIMO based on the Kalman criterion to reduce inter-user interference, evaluating both spectral and BER performance.

• **Proposed Approach:** We propose an iterative Kalman-based multi-user hybrid solution that minimizes the error between the preamble transmitted by the BS and the estimated received data at the MS.

We mathematically define the error formulation as a function of only the precoding, combining and channel matrices. In this way, the algorithm does not require any explicit data estimation. Then, a two step procedure is carried out: first, the RF analog precoding/combining step is performed as in single-user systems based on energy maximum principle; then an iterative Kalman-based approach is applied to estimate the digital baseband precoder at the BS in order to reduce inter-user interference.

• **Contributions:** The main contributions of this work are:

1) we devise a Kalman-based hybrid precoding/combining scheme for the discovery phase in multi-user mmWave massive MIMO systems, where the precoding baseband matrix is considered as the state matrix in the Kalman formulation;
2) we define the error between transmitted and estimated data as a function only of the precoding, combining and channel matrices, so that data estimation is not needed;
3) we show comparative simulation results both in terms of spectral efficiency and BER performance, which confirm that the proposed approach performs better than other existing hybrid solutions.

The paper is organized as follows: Sec. II describes the system model, Sec. III details the proposed Kalman formulation. Sec. IV presents the proposed Kalman hybrid analog/digital precoding algorithm, and Sec. V gives the simulations results. Finally, some concluding remarks are given in Sec. VI.

II. SYSTEM MODEL

For ease of explanation, we list the following notations that are used throughout the paper: $\mathbf{A}$ is a matrix, $\mathbf{a}$ is a vector, a is a scalar, and $\mathcal{A}$ is a set. $\|\mathbf{A}\|_F$ is the Frobenius norm of $\mathbf{A}$, whereas $\mathbf{A}^T$, $\mathbf{A}^H$, $\mathbf{A}^{-1}$ are its transpose, Hermitian, and inverse respectively. $\mathbf{I}$ is the identity matrix, and $\mathcal{N}(\mathbf{m}, \mathbf{R})$ is a complex Gaussian random vector with mean $\mathbf{m}$ and covariance $\mathbf{R}$. $E[\cdot]$ is used to denote expectation.

Differently from fully digital schemes, the number of RF chains may be much lower than the number of antennas in hybrid solutions [1], thus reducing the signal processing complexity and the energy consumption of RF chains. The network architecture is a mmWave-based massive MIMO cellular system where the BS is sending N_b streams through N_{BS} antennas and N_t RF chains for serving M mobile stations (MS), each with N_{MS} antennas and one RF chain, with $N_b < N_t < N_{BS}$ [12] [29]. Without loss of generality, we assume a simpler configuration of only one RF chain at the MS, similar to [12], [29], [35]. This assumption is justified since the implementation of user devices is influenced by the need for low complexity, cost, and power consumption. On the other hand, the BS may have more sophisticated digital signal processing (DSP) capability to support multiple concurrent data streams.

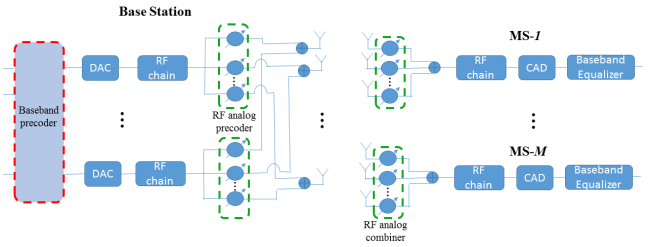

FIGURE 2. MmWave multi-user system with hybrid analog/digital precoding and analog combining.

The BS communicates with each MS via one stream, so that the total number of streams is $N_b = M$ and the maximum number of user M that can be served simultaneously by the BS is equal to the number of RF chains at the BS, that is $M \leq N_t$. Note that this architectural assumption is possible through the hybrid scheme, that allows spatial multiplexing and multi-user MIMO. In this way, the BS may communicate simultaneously with multiple MSs through multiple beams [1].

At the downlink, the BS sends a synchronization message applying both the baseband precoder $\mathbf{F}_{BB}$, with size $N_t \times N_b$, and the analog precoder $\mathbf{F}_{RF}$, with size $N_{BS} \times N_t$, so that the sampled transmitted signal is:

$$\mathbf{x} = \mathbf{F}_{RF}\mathbf{F}_{BB}\mathbf{s} \tag{1}$$

where $\mathbf{s}$ is the $N_b \times 1$ transmitted symbol vector, such that $E[\mathbf{s}\mathbf{s}^H] = \frac{P}{M}\mathbf{I}_M$, being P the transmitted power and $N_b = M$. We assume that P is equally allocated among different users' streams.

As highlighted in [20], following the same assumptions of [10], [36]–[39], for simplicity we adopt a narrowband block-fading channel.

Thus, the received signal at MS-m is:

$$\mathbf{r}_m = \mathbf{H}_m\mathbf{F}_{RF}\mathbf{F}_{BB}\mathbf{s} + \mathbf{n}_m \tag{2}$$

where $\mathbf{H}_m$ is the $N_{MS} \times N_{BS}$ matrix of the mmWave channel between the BS and the MS-m, and $\mathbf{n}_m \sim \mathcal{N}(\mathbf{0}, \sigma^2\mathbf{I})$ is the Gaussian noise vector.

The received signal $\mathbf{r}_m$ in (2) can be rewritten showing the desired contribution and the interference as follows:

$$\mathbf{r}_m = \mathbf{H}_m\mathbf{F}_{RF}\mathbf{f}_{BB_m}s_m + \mathbf{H}_m\sum_{j\neq m}^{M}\mathbf{F}_{RF}\mathbf{f}_{BB_j}s_j + \mathbf{n}_m \tag{3}$$

where $\mathbf{F}_{RF}\mathbf{f}_{BB_m}$ is the BS precoding vector for MS-m, $\mathbf{f}_{BB_m}$ is the column m of the matrix $\mathbf{F}_{BB}$. and s_j is the j^{th} element of $\mathbf{s}$.

Since the MS employ only RF analog combining $\mathbf{w}_{RF_m} = \mathbf{w}_m$, after the combining process, the estimated symbol of the MS-m can be expressed as:

$$\hat{s}_m = \mathbf{w}_m^H \mathbf{H}_m \mathbf{F}_{RF} \mathbf{F}_{BB} \mathbf{s} + \mathbf{w}_m^H \mathbf{n}_m \tag{4}$$

where $(\cdot)^H$ represents the conjugate transpose.

The estimated signal $\hat{s}_m$ in (4) can be written showing the desired contribution and the interference ones:

$$\hat{s}_m = \mathbf{w}_m^H \mathbf{H}_m \mathbf{F}_{RF} \mathbf{f}_{BB_m} s_m + \mathbf{w}_m^H \mathbf{H}_m \sum_{j \neq m}^{M} \mathbf{F}_{RF} \mathbf{f}_{BB_j} s_j + \mathbf{w}_m^H \mathbf{n}_m \tag{5}$$

On the uplink, the signal model is similar to (4) but the role of the precoders and combiners are exchanged. Hence, we replace $\mathbf{H}_m$ with $\mathbf{H}_m^T$, where $(\cdot)^T$ represents the transpose, using the principle of channel reciprocity [12].

Since mmWave channels show limited scattering [10], we use a geometric channel model with L_m scatterers for the m-th mobile station. Assuming that each scatterer contributes to a single propagation path between the BS and the MS-m [10], the channel $\mathbf{H}_m$ in (4) is expressed as

$$\mathbf{H}_m = \sqrt{\frac{N_{BS} N_{MS}}{L_m}} \sum_{l=1}^{L_m} \alpha_{m,l} \mathbf{a}_{MS}(\theta_{m,l}) \mathbf{a}_{BS}^H(\phi_{m,l}) \tag{6}$$

where $\alpha_{m,l}$ is the complex gain of the l-th path including the path loss between the BS and the MS-m, with $E[|\alpha_{m,l}|^2] = \bar{\alpha}$. The variables $\theta_{m,l}$ and $\phi_{m,l} \in [0, 2\pi]$ are the l-th path's angles of arrival and departure (AoAs/AoDs) respectively. $\mathbf{a}_{BS}(\phi_{m,l})$ and $\mathbf{a}_{MS}(\theta_{m,l})$ are the antenna array response vectors at the BS and MS-m, respectively.

If uniform linear arrays (ULA) are assumed at BS and MSs, $\mathbf{a}_{BS}(\phi_{m,l})$ can be expressed as:

$$\mathbf{a}_{BS}(\phi) = \frac{1}{N_{BS}} \left[1, \exp^{j\frac{2\pi}{\lambda} d \sin(\phi)}, \cdots, \exp^{j(N_{BS}-1)\frac{2\pi}{\lambda} d \sin(\phi)}\right] \tag{7}$$

where λ is the signal wavelength and d is the distance between antenna elements, and the array response vectors at the MS-m $\mathbf{a}_{MS}(\theta_{m,l})$ can be written in a similar way.

III. KALMAN FORMULATION FOR BEAMFORMING/COMBINING

Kalman filter [40], [41] is a powerful tool that has been exploited for several physical layer applications, such as carrier frequency synchronization [42], [43] and phase recovery [44], [45].

We next formulate the beamforming/combining problem using a Kalman filter-based approach, and then we propose a Kalman-based hybrid precoding solution. The system architecture consists of a hybrid analog/digital precoder at the BS, and simple MS devices with RF analog combining only.

The BS sends the preamble message $\mathbf{s}$, and the estimated signal $\hat{\mathbf{s}} = [\hat{s}_1, ..., \hat{s}_M]^T$ at the MS represents the observation vector, whose element $\hat{s}_m$ at MS-m can be defined at the iteration n as

$$\hat{s}_m(n) = (\mathbf{w}_m^H \mathbf{H}_m \mathbf{F}_{RF} \mathbf{F}_{BB}) \mathbf{s}(n) + \mathbf{n}_m(n) \tag{8}$$

where $\mathbf{s}(n)$ is the training vector transmitted from the BS as expressed in (1), and $\mathbf{w}_m^H \mathbf{H}_m \mathbf{F}_{RF} \doteq \mathbf{h}_m^H$ represents the effective downlink channel from the BS to MS-m, where $\mathbf{H}_e = [\mathbf{h}_1, ..., \mathbf{h}_M]^H$ is the effective channel matrix and represents the observer matrix.

The Kalman filter (KF) algorithm minimizes the sum-MSE $E\{\|\mathbf{s} - \hat{\mathbf{s}}\|^2\}$ of the training vector, defined as the squared difference between the signal $\mathbf{s}$ transmitted by the BS on different beams as expressed in (1), and the estimated signal $\hat{\mathbf{s}}$ at the MSs, that is the collection of all the estimates $\hat{s}_m$ represented in (8). The error $\mathbf{e}(n)$ at the n-th Kalman iteration is thus formulated as

$$\mathbf{e}(n) = \frac{\mathbf{s}(n) - \hat{\mathbf{s}}(n)}{\|\mathbf{s}(n) - \hat{\mathbf{s}}(n)\|_F^2} \tag{9}$$

We consider the baseband precoding matrix $\mathbf{F}_{BB}$ as the Kalman filter state, while the analog precoder $\mathbf{F}_{RF}$ is computed in the previous step of the algorithm 1 as detailed in Sec. IV-B.

The proposed Kalman state equation is given as follows:

$$\mathbf{F}_{BB}(n|n) = \mathbf{F}_{BB}(n|n-1) + \mathbf{K}(n) E\left\{\mathrm{diag}[\mathbf{e}(n)]\right\} \tag{10}$$

where $\mathbf{K}(n)$ represents the Kalman gains, and $\mathrm{diag}\left\{\mathbf{s}(n) - \hat{\mathbf{s}}(n)\right\}$ is the matrix representation of the error defined in (9), whose mean is computed using (8), and the effective channel representation $\mathbf{H}_e$, so that

$$E\left\{\mathrm{diag}[\mathbf{e}(n)]\right\} \frac{\mathbf{I} - \hat{\mathbf{H}}_e \mathbf{F}_{BB}(n|n-1)}{\|\mathbf{I} - \hat{\mathbf{H}}_e \mathbf{F}_{BB}(n|n-1)\|_F^2} \tag{11}$$

where $\hat{\mathbf{H}}_e$ is estimated as specified in Algorithm 1. Substituting (11) in (10) we obtain:

$$\mathbf{F}_{BB}(n|n) = \mathbf{F}_{BB}(n|n-1) + \mathbf{K}(n) \frac{\mathbf{I} - \hat{\mathbf{H}}_e \mathbf{F}_{BB}(n|n-1)}{\|\mathbf{I} - \hat{\mathbf{H}}_e \mathbf{F}_{BB}(n|n-1)\|_F^2} \tag{12}$$

In this way, the Kalman algorithm can be divided in the steps detailed in Sec. IV-C. The error in eq. (11) is normalized with respect its Frobenius norm.

Note that the observation vector $\hat{\mathbf{s}}(n)$ is needed for the formulation of the procedure, while, as detailed in the final formula (14) and (15)-(17) in Sec. IV, the algorithm at the BS does not require any details on the estimated data at the MSs, but only the precoding/combining matrices.

IV. KALMAN-BASED HYBRID PRECODING

In the hybrid multi-user system, we compute the analog combining $\mathbf{w}_m$ matrix for each mobile station and the hybrid analog and digital precoding $\mathbf{F}_{RF}$ and $\mathbf{F}_{BB}$ matrices at the BS.

A. HYBRID PRECODING OPTIMIZATION FORMULATION

We now aim to design the hybrid mmWave precoding matrix through the Kalman-based approach by minimizing the error defined in (9):

$$\begin{aligned} \underset{\mathbf{F}_{RF},\mathbf{F}_{BB}}{\text{minimize}} \quad & E\|\mathbf{s}-\hat{\mathbf{s}}\|^2 \\ \text{subject to} \quad & \|\mathbf{F}_{RF}\mathbf{F}_{BB}\|_F^2 \leq P \\ & \mathbf{F}_{RF} \in \{\mathbf{f}_1,...,\mathbf{f}_L\} \end{aligned} \tag{13}$$

where $\mathbf{s}(n)$ is the training vector $\mathbf{s}$ transmitted from the BS as expressed in (1), at the n-th Kalman iteration, and $\hat{\mathbf{s}}(n)$ is the collection $\hat{\mathbf{s}}$ of all the estimates $\hat{s}_m$ at MS-m expressed in (5) at iteration n.

The first condition $\|\mathbf{F}_{RF}\mathbf{F}_{BB}\|_F^2 \leq P$ in (13) refers to power constraint, while the second one is to limit the search for the columns of the RF precoder within a set of L basis vectors $\{\mathbf{f}_1,...,\mathbf{f}_L\}$. These basis vectors can be chosen from the transmit array response vectors at the angle of departure (AoD) of the mmWave channel, under the hypothesis of perfect AoD knowledge at the transmitter, or from a codebook $\mathcal{F}$ of quantized RF precoding vectors [10].

Given the error calculation in (11), the minimization problem (13) becomes

$$\begin{aligned} \underset{\mathbf{F}_{RF},\mathbf{F}_{BB}}{\text{minimize}} \quad & \|\mathbf{I}-\mathbf{H}_e\mathbf{F}_{BB}(n|n-1)\|_F^2 \\ \text{subject to} \quad & \|\mathbf{F}_{RF}\mathbf{F}_{BB}\|_F^2 \leq P \\ & \mathbf{F}_{RF} \in \{\mathbf{f}_1,...,\mathbf{f}_L\} \end{aligned} \tag{14}$$

The optimization formulation (14) does not involve any data transmission/estimation $\mathbf{s}(n)$ and $\hat{\mathbf{s}}(n)$ but only the precoding/combining matrices, i. e., $\mathbf{F}_{BB}$, $\mathbf{F}_{RF}$, and the collection of $\mathbf{w}_m$ contained in $\mathbf{H}_e$, that is the equivalent channel matrix defined as $\mathbf{H}_e = [\mathbf{h}_1,...,\mathbf{h}_M]^H$ in which $\mathbf{h}_m^H = \mathbf{w}_m^H\mathbf{H}_m\mathbf{F}_{RF}$ represents the effective downlink channel to MS-m in (8).

The problem (14) is nonconvex due to the multiplication of the variables $\mathbf{F}_{RF}$, $\mathbf{F}_{BB}$, and $\mathbf{w}_m$. However, if we fix $\mathbf{F}_{RF}$ and $\mathbf{w}_m$, we can solve the optimization problem and calculate $\mathbf{F}_{BB}$. Specifically, we first design the RF beamforming and combining matrices ($\mathbf{F}_{RF}$, $\mathbf{w}_m \forall m$) in Sec. IV-B, and then we compute the digital precoding $\mathbf{F}_{BB}$ through the iterative Kalman procedure in Sec. IV-C.

B. RF PRECODING AND COMBINING MATRIX

We determine first the RF beamforming/combining matrices for each BS-MS link independently, similarly to [12], and then continue with the baseband precoding to reduce the multi-user interference.

In the first step, the BS and each MS-m calculate the RF beamforming and combining vectors, $\mathbf{f}_{RF_m}$ and $\mathbf{w}_m$, by maximizing the signal power for the MS-m (line 3-6 in Algorithm 1). Existing single-user RF beamforming solutions can be used on this purpose [46] [47], in order to design the RF beamforming/combining vectors without explicit channel estimation and maintain a low training overhead.

Once the combining vectors $\mathbf{w}_m$ are determined for all MSs, as well as the the analog precoder $\mathbf{F}_{RF}$ at the BS, the digital baseband precoder $\mathbf{F}_{BB}$ is computed as follows.

C. ITERATIVE KALMAN BASEBAND PRECODING

At this step, the BS utilizes the effective channels $\mathbf{h}_m^H \doteq \mathbf{w}_m^H\mathbf{H}_m\mathbf{F}_{RF}\forall m$. Each effective channel vector $\mathbf{h}_m^H$ has dimension $M \times 1$, which is much lower than the original channel matrix $\mathbf{H}_m$ with size $N_{MS} \times N_{BS}$ [12]. Each MS-m uses a codebook $\mathcal{H}$ to quantize its effective channel response, and sends the index of the quantized channel vector to the BS (line 8-10 in Algorithm 1).

As the last step, the BS designs its Kalman-based digital precoder $\mathbf{F}_{BB}$ based on the quantized channels (line 11-18 in Algorithm 1). The sparse mmWave channels and the narrow beamforming ensure that the effective MIMO channel is well-conditioned [48]. This allows the Kalman-based digital beamforming approach to achieve near-optimal performance, as shown in Sec. V.

In particular, we consider $\mathbf{F}_{RF}$ with $\mathbf{w}_m$ calculated in Sec. IV-B. Thus, the Kalman algorithm can be incorporated in the following measurements update equations to compute $\mathbf{F}_{BB}$.

We calculate the conditional mean $\mathbf{F}_{BB}(n|n)$ and the variance $\mathbf{R}(n|n) = E[\mathbf{F}_{BB}(n)\mathbf{F}_{BB}^*(n)]$ of the state matrix $\mathbf{F}_{BB}(n)$, the Kalman gains $\mathbf{K}(n)$, at time instant n, according to (15), (16), and (17) respectively:

$$\mathbf{F}_{BB}(n|n) = \mathbf{F}_{BB}(n|n-1) + \mathbf{K}(n)\frac{\mathbf{I}-\mathbf{H}_D\mathbf{F}_{BB}(n|n-1)}{\|\mathbf{I}-\mathbf{H}_D\mathbf{F}_{BB}(n|n-1)\|_F^2} \tag{15}$$

$$\mathbf{K}(n) = \mathbf{R}(n|n-1)\mathbf{H}_D^H[\mathbf{H}_D\mathbf{R}(n|n-1)\mathbf{H}_D^H + \mathbf{Q}_n]^{-1} \tag{16}$$

$$\mathbf{R}(n|n) = [\mathbf{I}-\mathbf{K}(n)\mathbf{H}_D]\mathbf{R}(n|n-1) \tag{17}$$

where $\mathbf{H}_D$ is set equal to the equivalent channel matrix estimate $\hat{\mathbf{H}}_e$, and $\mathbf{Q}_n$ is the covariance matrix of the noise $\mathbf{n}(n)$. We set $\mathbf{Q}_n = (1/SNR) * \mathbf{I}$, where SNR is the signal to noise ratio. Although the proposed solution requires some iterations compared to the ZF [12] and MMSE [29] closed form equations, it gives better performance in adjusting the precoding matrix in a hybrid architecture. Moreover, as will be detailed in Sec. V, the number of needed iterations is limited to only few trials. Finally, we note that all the matrices involved in the Kalman formulation, i. e., $\mathbf{H}_D$, $\mathbf{K}$, $\mathbf{Q}_n$, and $\mathbf{R}$, have small size $M \times M$ where M is the number of users, and are independent from the large number of antennas N_{BS} and N_{MS} of the massive MIMO system.

The pseudo-code of the proposed Kalman-based hybrid precoding is summarized in the following Algorithm 1.

V. PERFORMANCE EVALUATION

In this section, we evaluate the performance of the proposed Kalman hybrid analog/digital precoding algorithm.

Algorithm 1 Kalman based hybrid beamforming

Input: BS RF codebook $\mathcal{F}$, MS RF codebook $\mathcal{W}$
Output: $\mathbf{F}_{BB}$, $\mathbf{F}_{RF}$, and $\mathbf{w}_m$ $\forall m = 1, ..., M$
Step 1 - RF Analog design: Single-user $\mathbf{F}_{RF}$ and $\mathbf{w}_m$ $\forall m$
  BS and MS-m select $\tilde{\mathbf{v}}_m, \tilde{\mathbf{g}}_m \forall m$ so that
  $\tilde{\mathbf{g}}_m, \tilde{\mathbf{v}}_m = \underset{\forall \mathbf{g}_m \in \mathcal{W}, \forall \mathbf{v}_m \in \mathcal{F}}{\arg\max} \|\mathbf{g}_m^H \mathbf{H}_m \mathbf{v}_m\|$
  BS sets $\mathbf{F}_{RF} = [\tilde{\mathbf{v}}_1, ..., \tilde{\mathbf{v}}_M]$ and MS-m sets $\mathbf{w}_m = \tilde{\mathbf{g}}_m \forall m$
Step 2 - BB Digital design: Multi-user $\mathbf{F}_{BB}$
  MS-m estimates $\tilde{\mathbf{h}}_m^H \doteq \mathbf{w}_m^H \mathbf{H}_m \mathbf{F}_{RF}$ and quantizes $\tilde{\mathbf{h}}_m$ using a codebook $\mathcal{H} \forall m$
  MS-m calculate and sends to BS $\hat{\mathbf{h}}_m$ $\forall m$ where
  $\hat{\mathbf{h}}_m = \underset{\hat{\mathbf{h}}_m \in \mathcal{H}}{\arg\max} \|\tilde{\mathbf{h}}_m^H \hat{\mathbf{h}}_m\|$
  BS sets $\mathbf{H}_D = \hat{\mathbf{H}}_e = [\hat{\mathbf{h}}_1, ..., \hat{\mathbf{h}}_M]^H$
  At BS: **for** $n \leq N$ **do**
    $\epsilon(n) = \frac{\mathbf{I} - \mathbf{H}_D \mathbf{F}_{BB}(n|n-1)}{\|\mathbf{I} - \mathbf{H}_D \mathbf{F}_{BB}(n|n-1)\|_F^2}$
    $\mathbf{F}_{BB}(n|n) = \mathbf{F}_{BB}(n|n-1) + \mathbf{K}(n)\epsilon(n)$
    $\mathbf{K}(n) = \mathbf{R}(n|n-1)\mathbf{H}_D^H [\mathbf{H}_D \mathbf{R}(n|n-1)\mathbf{H}_D^H + \mathbf{Q}_n]^{-1}$
    $\mathbf{R}(n|n) = [\mathbf{I} - \mathbf{K}(n)\mathbf{H}_D]\mathbf{R}(n|n-1)$
  Normalize $\mathbf{F}_{BB} = \sqrt{P} \frac{\mathbf{F}_{BB}}{\|\mathbf{F}_{RF}\mathbf{F}_{BB}\|_F}$

A. SIMULATION ENVIRONMENT

We consider the system described in Sec. II with a BS employing an 8×8 UPA and associated with 4 MSs, each having a 4×4 UPA, unless stated otherwise. Simulations are performed in Matlab© assuming both single-path channels ($L_m = 1$ in (6)), and multi-path channels ($L_m = 10$). The azimuth AoAs/AoDs are supposed to be uniformly distributed in $[0, 2\pi]$, the elevation AoAs/AoDs are uniformly distributed in $[-\pi/2, \pi/2]$, and perfect channel knowledge is assumed.

The performance of the proposed solution is shown in terms of the average achievable rates per user, $\mathbb{E}\left[\frac{1}{M}\sum_{m=1}^{M} A_m\right]$, with A_m:

$$A(m) = \log_2\left(1 + \frac{\frac{P}{M}\left|\mathbf{w}_m^H \mathbf{H}_m \mathbf{F}_{RF} \mathbf{f}_{BB_m}\right|^2}{\frac{P}{M}\sum_{n \neq m}\left|\mathbf{w}_m^H \mathbf{H}_m \mathbf{F}_{RF} \mathbf{f}_{BB_n}\right|^2 + \sigma^2}\right) \quad (18)$$

B. IMPACT OF VARYING SNR

Fig. 3 compares the rate achieved by the proposed hybrid Kalman precoding algorithm with the one obtained from simpler analog beamforming. Our study also examines the single-user rate (i. e., when there is no interference due to multi-user environment), and a fully-digital MSE beamforming. The figure illustrates the averaged achievable rates versus the SNR (signal to noise ratio) in multi-path scenario

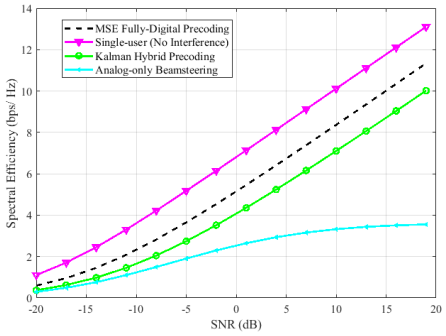

FIGURE 3. Achievable Rate varying SNR in multi-path scenario ($L_m = 10$) in the range $SNR = [-20, 20] dB$.

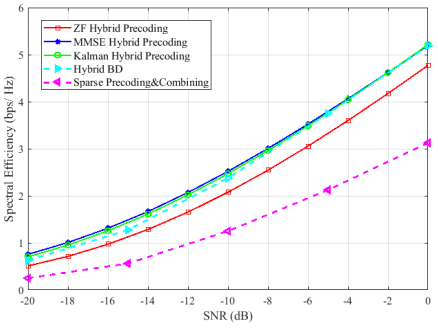

FIGURE 4. Comparison among hybrid precoding solutions: Achievable Rate varying SNR in the range $SNR = [-20, 20] dB$ with number of antennas $N_{BS} = 256$, number of MS antennas $N_{MS} = 64$, number of users $M = 8$.

($L_m = 10$). Results show that a classical analog-only solution is not sufficient, while the achievable rate obtained by the proposed scheme approaches close to the more complex fully-digital one. Moreover, the proposed hybrid algorithm is able to achieve performance closer to the single-user scenario, which means it is able to reduce the interference from the multi-user environment. Although sparse mmWave channels and large number of antennas at BS and MSs help in reducing multi-user interference, there is still a non-negligible amount of interference present [12].

Fig. 4 compares several hybrid solutions with the proposed Kalman based precoding scheme. Besides ZF [12] and MMSE [29], a hybrid block diagonalization (BD) algorithm [33] and a Sparse Precoding&Combining method [10] are included. In particular, the work [10] has been initially proposed for SU-MIMO and then extended to MU-MIMO in [33]. All the algorithms refer to the system architecture in the multipath scenario described in Sec. II, with multiple RF chains at the BS and one RF chain per user under the simulation setting [33]. The proposed Kalman based precoding shows the best performance along with the MMSE and Hybrid BD methods, while ZF spectral efficiency is lower due to its failure in multipath environment, as detailed in the following Fig. 5. Sparse Precoding&Combining method results in the lowest performance.

Fig. 5 compares the performance of the proposed hybrid

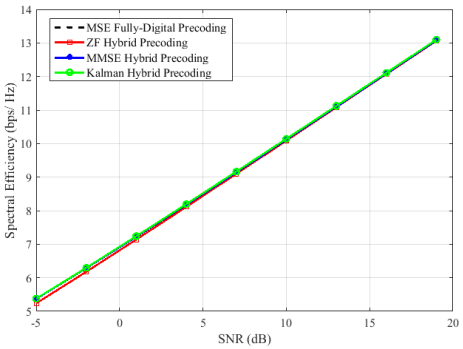

(a) Achievable rate in 1 path scenario

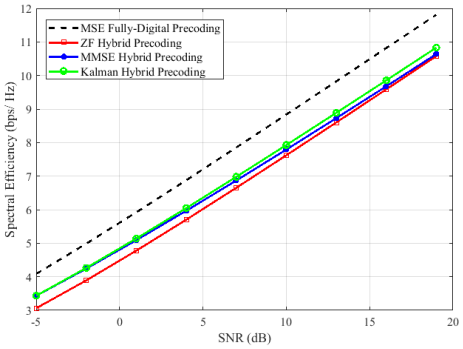

(b) Achievable rate in 5 paths scenario

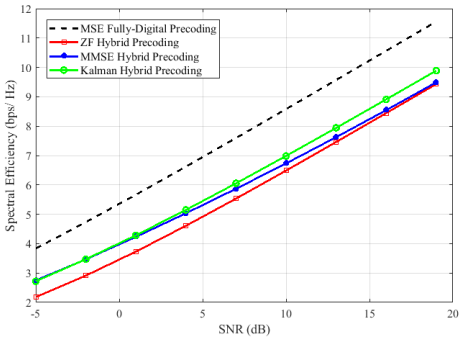

(c) Achievable rate in 10 paths scenario

FIGURE 5. Achievable Rate for Hybrid Precoding solutions varying SNR and the number of channel paths.

Kalman solution with other two hybrid schemes (ZF [12] and MMSE [29]) that consider the same system model, and a fully-digital MSE solution shown as a benchmark. Note that all the algorithms consider the same channel estimate.

In particular Fig. 5 shows different simulation scenarios, from single-path (Fig. 5(a)) to multi-path environment with a number of specific paths identified for closer scrutiny (Fig. 5(b)-5(c)). These particular cases are of interest, since mmWave channels are sparse, which means that only few paths exist [49]. While for a single-path scenario the three hybrid algorithms show similar performance (Fig. 5(a)), almost the same of the fully-digital one, when increasing the number of paths, their spectral efficiencies move away from the fully

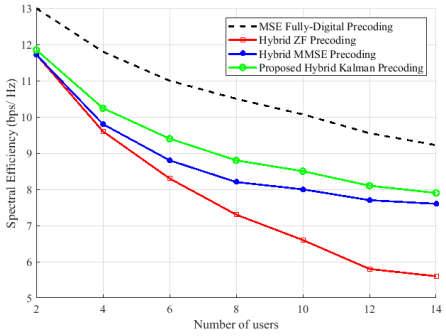

FIGURE 6. Achievable Rate varying the number of users with $SNR = 20dB$.

digital curve. However, the proposed hybrid Kalman solution outperforms both ZF and MMSE schemes (Fig. 5(b)-5(c)). In particular, ZF is the algorithm whose performance becomes worse in multipath environment, due to its lack in exploiting multipath channel gains. These latter scenarios are more realistic study cases, for recent measurement campaigns in mmWave bands reveal that the channels in a city environment can be well approximated with a pre-calculated number of paths clusters [50].

C. IMPACT OF NUMBER OF USERS

Fig. 6 presents the averaged achievable rates by varying the number of users for a fixed $SNR = 20dB$ in a multi-path scenario ($L_m = 10$). While the ZF procedure decrease its performance for higher number of users, both the proposed Kalman and MMSE algorithms show good outcomes with a similar trend, close to the fully digital bound. Anyway, the proposed Kalman solution is the algorithm that gives the best results. This is due to the iterative Kalman procedure that allows to better adjust the precoding baseband matrix, as well as the Kalman parameters, in a hybrid scheme. Note that only a small number of iterations is required, which we set as 10. We note that fewer iterations, i.e. 4-5, give similar results. The distance between the Kalman and fully-digital curve remains constant when increasing the number of users.

D. IMPACT OF THE NUMBER OF ANTENNAS

Fig. 7 shows the rates with different number of BS and MS antennas, assuming that $N_{BS} = N_{MS}$. When the number of antennas increases, the three hybrid solution show similar performance.

Given the implementation challenges and energy consumption limits, a practical considerations require higher number of antennas at the BS than at the MS. For this purpose, we simulate the scenario with a fixed number of MS antennas $N_{MS} = 16$ in Fig. 8, and a fixed number of BS antennas $N_{BS} = 64$ in Fig. 9, while varying the number of antennas at the BS and MS respectively.

Fig. 8 confirms the improvement of the proposed solutions for higher number of BS antennas (over the simple case of assuming $N_{BS} = N_{MS}$) as shown in Fig. 7.

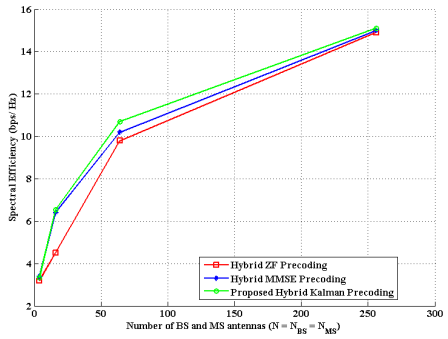

FIGURE 7. Achievable Rate varying the number of BS and MS antennas ($N = N_{BS} = N_{MS}$). $SNR = 20\ dB$ and 10 paths

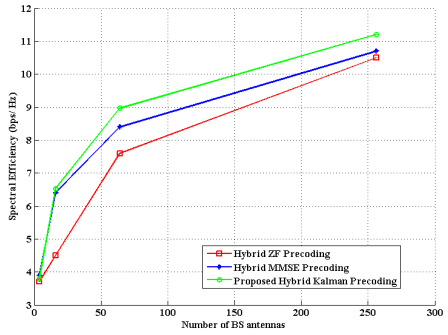

FIGURE 8. Achievable Rate varying the number of BS antennas N_{BS}. Number of MS antennas $N_{MS} = 16$, $SNR = 20\ dB$, $L_m = 10$ paths.

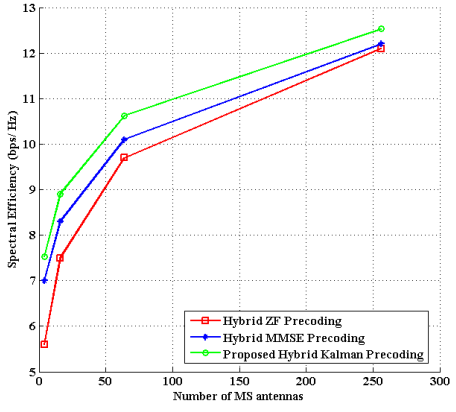

FIGURE 9. Achievable Rate varying the number of MS antennas. Number of BS antennas $N_{BS} = 64$, $SNR = 20\ dB$, $L_m = 10$ paths.

The trend from Fig. 8 also appears in Fig. 9 when varying the number of MS antennas. However, note that the case of the number of MS antennas being greater than BS antennas ($N_{MS} = 64$, $N_{MS} = 256$ in Fig. 9) may not be applied in practical cases.

Finally, Fig. 10, 11 illustrate the effect of the number of antennas on both the system architecture and the precoding schemes. We have included all the possible configuration scenarios, going from the practical setting $N_{BS} \geq N_{MS}$ to the theoretical case $N_{BS} < N_{MS}$, while varying the number of antennas to cover both MIMO and massive MIMO implementations.

In particular, Fig. 10(a) shows the rates when $N_{MS} = 4$ (solid lines), and when $N_{BS} = 4$ (dashed lines), with varying N_{BS} and N_{MS} respectively. In this way, we derive the insight that apart from the implementation ease and energy cost, it is better to have higher N_{BS} than N_{MS} also from the viewpoint of spectral efficiency. Moreover, in the practical case of N_{BS} higher than N_{MS} (solid lines) the proposed Kalman solution outperforms the other two hybrid schemes. In the opposite scenario of N_{BS} being lower than N_{MS} (dashed lines) the algorithms show similar, lower performance. This is due to the fact that increasing the number of antennas at the MS influences the analog combining, which is less efficient than the BS hybrid precoding. Moreover, in the simulation study, the MS combining vectors are assumed the same for the three algorithms. Thus, the performance of the hybrid algorithms improves more when increasing the number of BS antennas than the MS ones. Additionally, the difference among the algorithms' performance are more evident.

Similar to the studies in Fig. 10(a), in Fig. 10(b)-11(b) we increase the fixed number of antennas to 16, 64 and 256, respectively. In particular, Fig. 10(b) shows two simulation settings, the first one with $N_{MS} = 16$ (solid lines) and the second one with $N_{BS} = 16$ (dashed lines). Similarly Fig. 11(a) has $N_{MS} = 64$ (solid lines) and $N_{BS} = 64$ (dashed lines), and Fig. 11(b) has $N_{MS} = 256$ (solid lines) and $N_{BS} = 256$ (dashed lines).

Comparing Fig. 10(a) and Fig. 10(b), when increasing the number of fixed antennas from 4 (Fig. 10(a)) to 16 (Fig. 10(b)), the gap between solid and dashed lines decreases and hence this lowers the spectral efficiency gain. This is simply due to the lower difference between the number of antennas in this new setting. As an example, let us consider in Fig. 10(a) the point of the green solid line for $N_{MS} = 4$ and $N_{BS} = 64$ that has spectral efficiency equal to 7.5 bps/Hz, which becomes 4.4 bps/Hz for the dashed green line. In this way there is a gain of 3.1 bps/Hz for a difference $N_{BS_{solid}} - N_{BS_{dashed}} = 60$. In Fig. 10(b) the gap becomes $9 - 7.8 = 2.2\ bps/Hz$ due to the difference $N_{BS_{solid}} - N_{BS_{dashed}} = 48$ lower than 60 as in Fig. 10(a). Anyhow, the better behavior of the proposed Kalman solution is confirmed also in such scenario.

In Fig. 11(a) both the spectral efficiency gain of having N_{BS} higher than N_{MS} and the gain of the Kalman algorithm over the other two hybrid solutions decrease, since the abso-

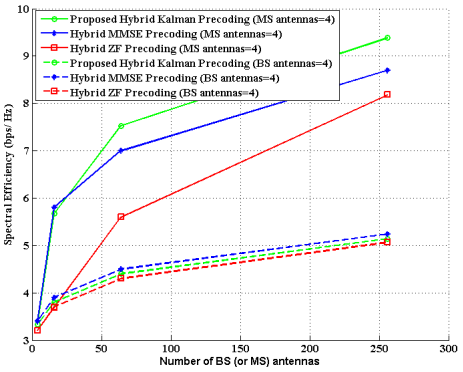

(a) Achievable rate when MS (or BS) antennas are fixed to 4

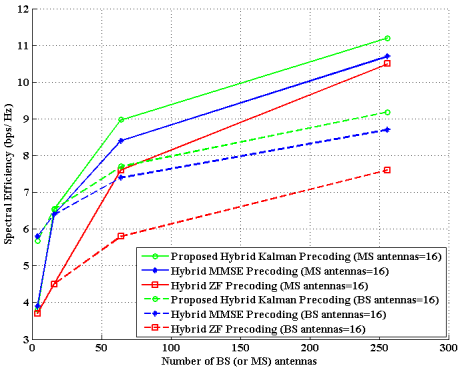

(b) Achievable rate when MS (or BS) antennas are fixed to 16

FIGURE 10. Achievable Rate for Hybrid Precoding when the number of BS (or MS) antennas are fixed to a certain value. $SNR = 20dB$ and 10 paths.

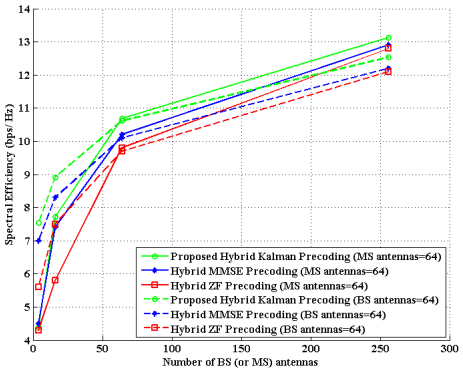

(a) Achievable rate when MS (or BS) antennas are fixed to 64

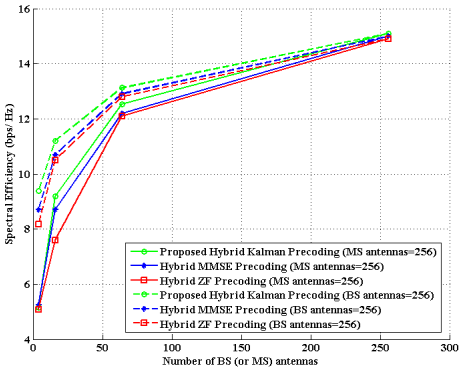

(b) Achievable rate when MS (or BS) antennas are fixed to 256

FIGURE 11. Achievable Rate for Hybrid Precoding when the number of BS (or MS) antennas are fixed to a certain value. $SNR = 20dB$ and 10 paths.

lute value of the difference $N_{BS_{solid}} - N_{BS_{dashed}}$ is lower than in the previous figures.

Finally, in Fig. 11(b), when N_{BS} (or N_{MS}) is high, equal to 256, the position of dashed and solid lines is inverted compared to the previous Fig. 10(a)-11(a), confirming the advantage of having an higher number of antennas at the BS than at the MSs. The trend of the hybrid precoding scheme is always the same, although the difference performance of the Kalman solution compared to the other two algorithms is less evident.

As a practical configuration implies higher number of antennas at the BS than at MS, as in Fig. 10(a) and 10(b), we see the performance of the proposed Kalman solution is much better compared to the other schemes.

E. BER PERFORMANCE EVALUATION

Fig. 12 compares BER performance of different schemes for QPSK modulation in the simulation setting [35]. Hybrid tree search method [35] calculates the optimal beam subset via a tree search, while maximum magnitude (MM) algorithm [51] selects the beams that allows the maximum received power for each MS. The proposed Kalman solution shows the best performance, which however is closed to the MMSE

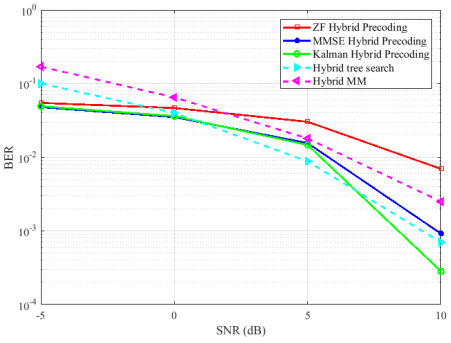

FIGURE 12. BER evaluation with number of BS antennas $N_{BS} = 64$, number of MS antennas $N_{MS} = 4$, number of users $M = 4$.

and hybrid tree search ones. Poor ZF trend is due to its failure in multipath scenario as detailed in Fig. 5, while the low MM performance depends on its inability to accurately choose the beam subset that has produced performance loss.

VI. CONCLUSION

We proposed a multi-user beamforming solution for mmWave massive MIMO systems, based on a Kalman formulation and a hybrid precoding designed by minimizing

the error between the transmitted and estimated data. The method uses a specially designed formulation of the error, and following this, a two-step procedure is carried out to first calculate the RF precoding/combining matrix, and then design the digital baseband precoder at the BS.

Simulation results show that the proposed algorithm outperforms existing solutions, in terms of both spectral efficiency and BER, due to its ability to better adjust the precoding matrix in hybrid architectures. In future work, we will incorporate a channel estimation scheme in the Kalman hybrid precoding algorithm, and extend the proposed solution to mobile scenarios. Moreover, we will focus on extending the proposed solution to joint precoders/combiners iterative optimization [52] when user devices employ multiple streams.

REFERENCES

[1] R. W. Heath, N. González-Prelcic, S. Rangan, W. Roh, and A. M. Sayeed, "An overview of signal processing techniques for millimeter wave mimo systems," IEEE Journal of Selected Topics in Signal Processing, vol. 10, no. 3, pp. 436–453, April 2016.

[2] M. E. Özçevik, B. Canberk, and T. Q. Duong, "End to end delay modeling of heterogeneous traffic flows in software defined 5g networks," Ad Hoc Networks, vol. 60, no. Supplement C, pp. 26 – 39, 2017. [Online]. Available: http://www.sciencedirect.com/science/article/pii/S1570870517300422

[3] J. G. Andrews, S. Buzzi, W. Choi, S. V. Hanly, A. Lozano, A. C. K. Soong, and J. C. Zhang, "What Will 5G Be?" IEEE Journal on Selected Areas in Communications, vol. 32, no. 6, pp. 1065–1082, June 2014.

[4] V. Petrov, M. Komarov, D. Moltchanov, J. M. Jornet, and Y. Koucheryavy, "Interference and sinr in millimeter wave and terahertz communication systems with blocking and directional antennas," IEEE Transactions on Wireless Communications, vol. 16, no. 3, pp. 1791–1808, March 2017.

[5] T. Yilmaz, G. Gokkoca, and O. B. Akan, Millimetre Wave Communication for 5G IoT Applications. Cham: Springer International Publishing, 2016, pp. 37–53. [Online]. Available: https://doi.org/10.1007/978-3-319-30913-2_3

[6] V. Wong, S. R., D. Ng, and W. L., Key Technologies for 5G Wireless Systems. Cambridge University Press, 2017.

[7] F. Boccardi, R. W. Heath, A. Lozano, T. L. Marzetta, and P. Popovski, "Five disruptive technology directions for 5g," IEEE Communications Magazine, vol. 52, no. 2, pp. 74–80, February 2014.

[8] I. F. Akyildiz, W.-Y. Lee, M. C. Vuran, and S. Mohanty, "Next generation/dynamic spectrum access/cognitive radio wireless networks: A survey," Computer Networks, vol. 50, no. 13, pp. 2127 – 2159, 2006. [Online]. Available: http://www.sciencedirect.com/science/article/pii/S1389128606001009

[9] S. K. Saha, D. G. Malleshappa, A. Palamanda, V. V. Vira, A. Garg, and D. Koutsonikolas, "60 ghz indoor wlans: insights into performance and power consumption," Wireless Networks, Mar 2017. [Online]. Available: https://doi.org/10.1007/s11276-017-1475-4

[10] O. E. Ayach, S. Rajagopal, S. Abu-Surra, Z. Pi, and R. W. Heath, "Spatially sparse precoding in millimeter wave mimo systems," IEEE Transactions on Wireless Communications, vol. 13, no. 3, pp. 1499–1513, March 2014.

[11] A. Alkhateeb, R. W. Heath, and G. Leus, "Achievable rates of multi-user millimeter wave systems with hybrid precoding," in 2015 IEEE International Conference on Communication Workshop (ICCW), June 2015, pp. 1232–1237.

[12] A. Alkhateeb, G. Leus, and R. W. Heath, "Limited feedback hybrid precoding for multi-user millimeter wave systems," IEEE Transactions on Wireless Communications, vol. 14, no. 11, pp. 6481–6494, Nov 2015.

[13] W. Roh, J. Y. Seol, J. Park, B. Lee, J. Lee, Y. Kim, J. Cho, K. Cheun, and F. Aryanfar, "Millimeter-wave beamforming as an enabling technology for 5g cellular communications: theoretical feasibility and prototype results," IEEE Communications Magazine, vol. 52, no. 2, pp. 106–113, February 2014.

[14] R. MÃl'ndez-Rial, C. Rusu, N. GonzÃąlez-Prelcic, A. Alkhateeb, and R. W. Heath, "Hybrid mimo architectures for millimeter wave communications: Phase shifters or switches?" IEEE Access, vol. 4, pp. 247–267, 2016.

[15] H. Li, Z. Wang, Q. Liu, and M. Li, "Transmit Antenna Selection and Analog Beamforming with Low-Resolution Phase Shifters in mmWave MISO Systems," IEEE Communications Letters, pp. 1–1, 2018.

[16] X. Li, Y. Zhu, and P. Xia, "Enhanced Analog Beamforming for Single Carrier Millimeter Wave MIMO Systems," IEEE Transactions on Wireless Communications, vol. 16, no. 7, pp. 4261–4274, July 2017.

[17] M. Jasim, J. E. Pezoa, and N. Ghani, "Simultaneous multi-beam analog beamforming and coded grating lobes for initial access in mmWave systems," in 2017 CHILEAN Conference on Electrical, Electronics Engineering, Information and Communication Technologies (CHILECON), Oct 2017, pp. 1–6.

[18] M. Lee and W. Chung, "Transmitter design for analog beamforming aided spatial modulation in millimeter wave MIMO systems," in 2016 IEEE 27th Annual International Symposium on Personal, Indoor, and Mobile Radio Communications (PIMRC), Sept 2016, pp. 1–6.

[19] S. Hur, T. Kim, D. J. Love, J. V. Krogmeier, T. A. Thomas, and A. Ghosh, "Millimeter wave beamforming for wireless backhaul and access in small cell networks," IEEE Transactions on Communications, vol. 61, no. 10, pp. 4391–4403, October 2013.

[20] D. H. N. Nguyen, L. B. Le, T. Le-Ngoc, and R. W. Heath, "Hybrid mmse precoding and combining designs for mmwave multiuser systems," IEEE Access, vol. 5, pp. 19 167–19 181, 2017.

[21] A. F. Molisch, V. V. Ratnam, S. Han, Z. Li, S. L. H. Nguyen, L. Li, and K. Haneda, "Hybrid beamforming for massive mimo: A survey," IEEE Communications Magazine, vol. 55, no. 9, pp. 134–141, 2017.

[22] R. Magueta, D. Castanheira, A. Silva, R. Dinis, and A. Gameiro, "Non linear space-time equalizer for single-user hybrid mmWave massive MIMO systems," in 2016 8th International Congress on Ultra Modern Telecommunications and Control Systems and Workshops (ICUMT), Oct 2016, pp. 177–182.

[23] J. Zhang, A. Wiesel, and M. Haardt, "Low rank approximation based hybrid precoding schemes for multi-carrier single-user massive MIMO systems," in 2016 IEEE International Conference on Acoustics, Speech and Signal Processing (ICASSP), March 2016, pp. 3281–3285.

[24] S. Han, C. I, Z. Xu, and C. Rowell, "Large-scale antenna systems with hybrid analog and digital beamforming for millimeter wave 5G," IEEE Communications Magazine, vol. 53, no. 1, pp. 186–194, January 2015.

[25] C. Kim, T. Kim, and J. Seol, "Multi-beam transmission diversity with hybrid beamforming for MIMO-OFDM systems," in 2013 IEEE Globecom Workshops (GC Wkshps), Dec 2013, pp. 61–65.

[26] X. Zhang, A. F. Molisch, and S.-Y. Kung, "Variable-phase-shift-based rf-baseband codesign for mimo antenna selection," IEEE Transactions on Signal Processing, vol. 53, no. 11, pp. 4091–4103, Nov 2005.

[27] V. Venkateswaran and A. J. van der Veen, "Analog beamforming in mimo communications with phase shift networks and online channel estimation," IEEE Transactions on Signal Processing, vol. 58, no. 8, pp. 4131–4143, Aug 2010.

[28] L. Zhao, D. W. K. Ng, and J. Yuan, "Multi-User Precoding and Channel Estimation for Hybrid Millimeter Wave Systems," IEEE Journal on Selected Areas in Communications, vol. 35, no. 7, pp. 1576–1590, July 2017.

[29] D. H. N. Nguyen, L. B. Le, and T. Le-Ngoc, "Hybrid mmse precoding for mmwave multiuser mimo systems," in 2016 IEEE International Conference on Communications (ICC), May 2016, pp. 1–6.

[30] Z. Wang, M. Li, X. Tian, and Q. Liu, "Iterative hybrid precoder and combiner design for mmwave multiuser mimo systems," IEEE Communications Letters, vol. 21, no. 7, pp. 1581–1584, July 2017.

[31] J. Mao, Z. Gao, Y. Wu, and M. Alouini, "Over-Sampling Codebook-Based Hybrid Minimum Sum-Mean-Square-Error Precoding for Millimeter-Wave 3D-MIMO," IEEE Wireless Communications Letters, pp. 1–1, 2018.

[32] J. Li, L. Xiao, X. Xu, and S. Zhou, "Robust and Low Complexity Hybrid Beamforming for Uplink Multiuser MmWave MIMO Systems," IEEE Communications Letters, vol. 20, no. 6, pp. 1140–1143, June 2016.

[33] W. Ni and X. Dong, "Hybrid Block Diagonalization for Massive Multiuser MIMO Systems," IEEE Transactions on Communications, vol. 64, no. 1, pp. 201–211, Jan 2016.

[34] C. Hu, J. Liu, X. Liao, Y. Liu, and J. Wang, "A novel equivalent baseband channel of hybrid beamforming in massive multiuser mimo systems," IEEE Communications Letters, vol. 22, no. 4, pp. 764–767, April 2018.

[35] L. Lin, W. Chung, H. Chen, and T. Lee, "Energy Efficient Hybrid Precoding for Multi-User Massive MIMO Systems Using Low-Resolution

ADCs," in 2016 IEEE International Workshop on Signal Processing Systems (SiPS), Oct 2016, pp. 115–120.
[36] A. Alkhateeb, O. E. Ayach, G. Leus, and R. W. Heath, "Channel estimation and hybrid precoding for millimeter wave cellular systems," IEEE Journal of Selected Topics in Signal Processing, vol. 8, no. 5, pp. 831–846, Oct 2014.
[37] E. Torkildson, C. Sheldon, U. Madhow, and M. Rodwell, "Millimeter-wave spatial multiplexing in an indoor environment," in 2009 IEEE Globecom Workshops, Nov 2009, pp. 1–6.
[38] J. Brady, N. Behdad, and A. M. Sayeed, "Beamspace mimo for millimeter-wave communications: System architecture, modeling, analysis, and measurements," IEEE Transactions on Antennas and Propagation, vol. 61, no. 7, pp. 3814–3827, July 2013.
[39] P. Xia, S. K. Yong, J. Oh, and C. Ngo, "A practical sdma protocol for 60 ghz millimeter wave communications," in 2008 42nd Asilomar Conference on Signals, Systems and Computers, Oct 2008, pp. 2019–2023.
[40] R. E. Kalman, "A New Approach to Linear Filtering and Prediction Problems," Transaction of the ASME Journal of Basic Engineering, vol. 82, no. 1, pp. 35–45, 1960.
[41] S. Haykin, Kalman Filtering and Neural Networks. New York, NY, USA: John Wiley & Sons, Inc., 2001.
[42] A. Câmpeanu and J. Gál, "Kalman filter carrier synchronization algorithm," in 2012 10th International Symposium on Electronics and Telecommunications, Nov 2012, pp. 203–208.
[43] W. Lin and D. Chang, "Adaptive Carrier Synchronization Using Decision-Aided Kalman Filtering Algorithms," IEEE Transactions on Consumer Electronics, vol. 53, no. 4, pp. 1260–1267, Nov 2007.
[44] A. Vizziello, P. Savazzi, and R. Borra, "Joint Phase Recovery for XPIC System Exploiting Adaptive Kalman Filtering," IEEE Communications Letters, vol. 20, no. 5, pp. 922–925, May 2016.
[45] F. Kulsoom, A. Vizziello, R. Borra, and P. Savazzi, "Reduced complexity Kalman filtering for phase recovery in XPIC systems," Physical Communication, vol. 29, pp. 112 – 119, 2018.
[46] J. Wang, Z. Lan, C.-W. Pyo, T. Baykas, C.-S. Sum, M. A. Rahman, J. Gao, R. Funada, F. Kojima, H. Harada, and S. Kato, "Beam codebook based beamforming protocol for multi-gbps millimeter-wave wpan systems," IEEE Journal on Selected Areas in Communications, vol. 27, no. 8, pp. 1390–1399, October 2009.
[47] S. Hur, T. Kim, D. J. Love, J. V. Krogmeier, T. A. Thomas, and A. Ghosh, "Millimeter wave beamforming for wireless backhaul and access in small cell networks," IEEE Transactions on Communications, vol. 61, no. 10, pp. 4391–4403, October 2013.
[48] P. J. Smith, C. Neil, M. Shafi, and P. A. Dmochowski, "On the convergence of massive mimo systems," in 2014 IEEE International Conference on Communications (ICC), June 2014, pp. 5191–5196.
[49] T. S. Rappaport, S. Sun, R. Mayzus, H. Zhao, Y. Azar, K. Wang, G. N. Wong, J. K. Schulz, M. Samimi, and F. Gutierrez, "Millimeter wave mobile communications for 5g cellular: It will work!" IEEE Access, vol. 1, pp. 335–349, 2013.
[50] M. R. Akdeniz, Y. Liu, M. K. Samimi, S. Sun, S. Rangan, T. S. Rappaport, and E. Erkip, "Millimeter wave channel modeling and cellular capacity evaluation," IEEE Journal on Selected Areas in Communications, vol. 32, no. 6, pp. 1164–1179, June 2014.
[51] P. V. Amadori and C. Masouros, "Low RF-Complexity Millimeter-Wave Beamspace-MIMO Systems by Beam Selection," IEEE Transactions on Communications, vol. 63, no. 6, pp. 2212–2223, June 2015.
[52] Z. Wang, M. Li, X. Tian, and Q. Liu, "Iterative hybrid precoder and combiner design for mmwave multiuser mimo systems," IEEE Communications Letters, vol. 21, no. 7, pp. 1581–1584, July 2017.

ANNA VIZZIELLO received the Laurea degree in Electronic Engineering and the Ph.D. degree in Electronics and Computer Science from the University of Pavia, Italy, in 2007 and in 2011, respectively.

She is currently a research fellow in the Telecommunication & Remote Sensing Laboratory at the University of Pavia, Italy. From 2007 to 2009 she also collaborated with European Centre for Training and Research in Earthquake Engineering (EUCENTRE) working in the Telecommunications and Remote Sensing group. From 2009 to 2010 she has been a visiting researcher at Broadband Wireless Networking Lab at Georgia Institute of Technology, Atlanta, GA, in summer 2009 and 2010 at Universitat Politècnica de Catalunya, Barcelona, Spain, and in winter 2011 and in summer 2016 at Northeastern University, Boston MA. Her research interests are Cognitive Radio Networks, 5G Systems, Intra-body Networks.

PIETRO SAVAZZI received the Laurea degree in Electronics Engineering and the Ph.D. degree in Electronics and Computer Science from the University of Pavia, Italy, in 1995 and in 1999, respectively.

In 1999, he joined Ericsson Lab Italy, in Milan, as a system designer, working on broadband microwave systems. In 2001 he moved to Marconi Mobile, Genoa, Italy, as a system designer in the filed of 3G wireless systems. Since 2003 he has been working at the University of Pavia where he is currently teaching, as an assistant professor, two courses on signal processing and wireless sensor networks. His main research interests are in wireless communication and sensor systems.

PROF. KAUSHIK R. CHOWDHURY received the PhD degree from the Georgia Institute of Technology, Atlanta, in 2009.

He is currently Associate Professor and Faculty Fellow in the Electrical and Computer Engineering Department at Northeastern University, Boston, MA. He was awarded the Presidential Early Career Award for Scientists and Engineers (PECASE) in Jan. 2017, the DARPA Young Faculty Award in 2017, the Office of Naval Research Director of Research Early Career Award in 2016, and the NSF CAREER award in 2015. He received multiple best paper awards, including the IEEE INFOCOM 2018, the IEEE ICC conference, in 2009, '12 and '13, and ICNC conference in 2013. He is presently a co-director of the Platforms for Advanced Wireless Research project office, a joint $ 100 million public-private investment partnership between the US NSF and wireless industry consortium to create city-scale testing platforms.